3rd Specialty Conference on Material Engineering & Applied Mechanics
3e Conférence spécialisée sur le génie des matériaux et mécanique appliquée

Montréal, Québec
May 29 to June 1, 2013 / *29 mai au 1 juin 2013*

ADVANCED COMPUTATIONAL STRESS ANALYSIS OF A STRANDED OVERHEAD LINE CONDUCTOR UNDER FRETTING FATIGUE CONDITIONS

G. Qi[1] and G. McClure[2]
[1] Ph.D. Candidate, E-mail: Gang.Qi@mail.mcgill.ca
[2] Associate Professor, E-mail: Ghyslaine.McClure@mcgill.ca
Department of Civil Engineering and Applied Mechanics, McGill University, Montreal, Canada

ABSTRACT: Fretting fatigue of stranded conductors is widely acknowledged as a critical problem in electric utilities as it contributes to significant degradation of local fatigue strength of transmission line conductors, leading to drastic reduction of their service life. However, fretting fatigue behavior of conductor wires cannot be well predicted and characterized by either experimental testing or simplified theoretical models, owing to the synthetic geometry, material and loading complexities. Therefore, reliable computational models have been long expected. Nevertheless, helically stranded cable geometries, nonlinear material properties, substantial friction effects, and comprehensive contact interactions have made the task very challenging. This paper presents the nonlinear finite element (FE) stress analysis of an ACSR conductor-clamp system to describe the detailed mechanical response of stranded conductors under fretting fatigue conditions, from an applied mechanics perspective. A 3-D elastic-plastic, large deformation, multi-body frictional contact FE model was constructed and implemented as a multiple-load-step analysis to complete the load history of one fretting cycle. The FE model comprises all structural components of the conductor-clamp system - an ACSR conductor with 33 helical wires, a suspension clamp body, and its upper keeper and U-bolt - adding up to nearly 324,000 nodes, 310,000 solid elements and 274,500 contact elements. The salient features of FE modeling and numerical solution techniques for solving this highly nonlinear large model are discussed in detail, from which a faithful modeling methodology is developed and validated. The computational results show good agreement with some experimental measurements and field observations reported in the open literature.

1. INTRODUCTION

Overhead line (OHL) conductors are exposed mainly to several sources of static loads in their normal service: constant axial tension from installation and span weight; local compressive forces exerted by clamping devices; an internal torque is also induced by the axial tension which tends to unwind the conductor. In the past, extensive research efforts have been made to understand mainly the mechanical (static and dynamic) response of stranded conductors under the limit design environment. During most of their lifespan, however, conductors are subjected to these operational loads that are only a fraction of their peak design requirements, and meanwhile conductor fatigue has been widely recognized as the most dangerous threat to conductor reliability. Aeolian vibrations of conductors (of low amplitude and high frequency) are among the most detrimental factors that drastically reduce the conductor service life. These oscillations cause longitudinal tension fluctuations that promote fretting fatigue failure of individual wires and eventually entire conductor strand breakage in highly constrained suspension clamp regions.

Numerous laboratory tests on conductor fretting fatigue were performed over the past decades. Although some general behavioral trends can be confirmed with experimental studies (see for example, Zhou et al., 1994, 1995, 1996), it is acknowledged that fretting fatigue response of conductor wires is very difficult to predict and characterize owing to their synthetic geometry, material and loading complexities. For

instance, wire fractures have been observed on either external or internal layers depending on different testing conditions. Also, fretting crack propagations may proceed by several modes and have different contributions to total fatigue life. From a structural mechanics perspective, accurate description and prediction of the conductor wire stress states at the clamp mouth region are essential to provide a clear explanation of the mechanical behavior of stranded conductors under fretting fatigue conditions and to identify fatigue damage initiation (fretting crack nucleation). Accuracy of stress analysis models is particularly important because small stress variations (by only a small percentage) can translate into significant differences in the assessment of the fatigue life of overhead conductors. The complex stresses states in individual conductor wires as well as those at the interface between the external wires and the clamp surfaces are not accessible to direct measurements, while simplified theoretical models based on semi-empirical formulae and linear elastic assumptions can only yield idealized nominal stresses that may be very different that the actual stress states. Therefore, reliable computational models for stress analysis have been long expected to achieve accurate stress predictions. It is anticipated that such models, in combination with the large amount of experimental data generated over the last decades, will contribute to resolve these long-lasting issues of conductor fretting fatigue and general vibration-induced damage that are critical for OHL design and maintenance. Nevertheless, detailed and accurate numerical modeling of conductor fretting fatigue remains a daunting task due to the computational uncertainty, complexity and high-nonlinearity (Azevedo et al., 2009).

To the authors' knowledge, no comprehensive numerical work is available in the published literature that presents a rational mechanics-based model to describe the fretting fatigue phenomena in electrical stranded conductors. Hence, the objective of the present study is to fill this knowledge gap, by developing a faithful computational approach model to explore the mechanical response of a typical conductor-clamp system under bending fretting fatigue conditions. The approach is illustrated with a detailed conductor/clamp example where local stress and strain fields in the suspension clamp mouth regions of fretting are predicted by detailed 3-D elastic-plastic multi-body contact analyses with friction. This paper will focus mainly on the numerical challenges encountered during modeling. The main analysis procedures and key numerical solution techniques used in the study are discussed. Computational results and some numerical findings could be validated by comparison with published experimental data and field observations.

2. THREE-DIMENSIONAL SOLID MODELING

Laboratory tests have shown that different fretting conditions may have significant influences on conductor fretting crack nucleation and propagation, depending on material properties, contact geometry configurations and loading conditions, as well as their compounded effects. Accordingly, for the purpose of developing a stress analysis methodology, the numerical model needs to correspond to a particular conductor-clamp system.

First of all, the commonly used "envelope type" suspension clamp is chosen (see Figure 1). A suspension clamp assembly typically comprises a lower clamp body with a lengthwise groove for receiving the lower side of the conductor, an elongated upper keeper to restrain the upper side of the conductor, as well as two U-bolts and nuts that connect the clamp-conductor assembly. The suspension clamp assembly is a critical device as it imposes severe constraints on the conductor due to its rigidity and clamping force. A suspension clamp is pinned to the supporting tower such that the conductor/clamp system is free to swing longitudinally (as a rigid body) under the unbalanced tensions induced in conductors due to environmental loads. However, when conductors vibrate, the global effect is conductor bending relative to the clamp assembly, with maximum bending moment at the keeper edge. From a fretting fatigue point of view, the critical conductor zone is located between the keeper edge (KE) and the clamp body last point of contact (LPC). Hence the lengths of the clamp body and the keeper are two key parameters that have significant effects on contact stresses, fretting regions and crack initiation. In accordance with the experimental work by Zhou et al. (1994, 1995), a generic "envelope type" suspension clamp assembly is adopted here with a 216 mm clamp body and a 124 mm keeper, measured from the suspension clamp axis. The clamp body and keeper are both made of permanent mould-cast aluminum.
A two-layer 795 kcmil (26/7) "Drake" type ACSR bare conductor is selected as a benchmark conductor due to its wide use throughout the electric utility industry. As illustrated in Figures 2 and 3, it is a

composite concentric-lay-stranded cable, comprising a steel central core (a 7-wire concentric helical strand) surrounded by two layers (16 outer wires and 10 inner wires) of helically wound aluminum alloy strands with opposite helical directions. The external diameter of the bare conductor is 28.133 mm. The precision of the conductor solid model does affect significantly the accuracy of the contact interactions among the wires, the mesh size and the stress results. In this study, the conductor solid model is built with as much geometrical accuracy as possible, using the design specifications as described in details in Qi (2013).

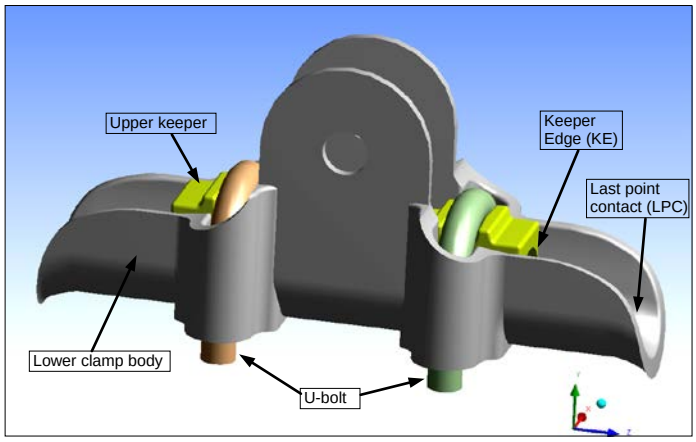

Figure 1: The suspension clamp assembly solid model

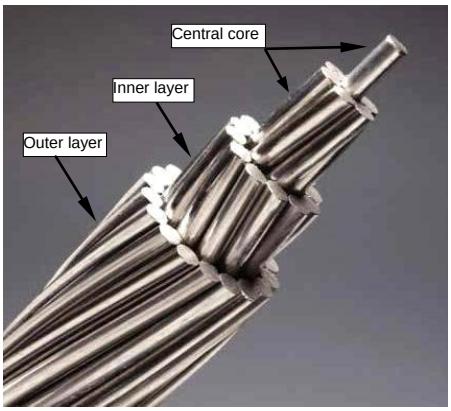

Figure 2: Drake conductor configuration

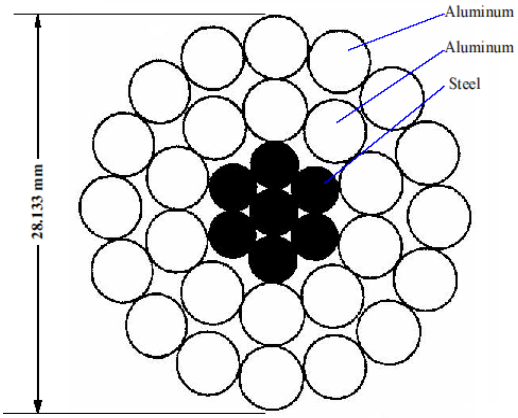

Figure 3: Drake schematic cross-section

The bending fretting fatigue testing rig setup used as reference is the one used by Azevedo et al. (2009), which is in compliance with the IEEE standard (1966) and EPRI Transmission Line Reference Book (1979, 2006), see Figure 4. The test is controlled by an imposed vertical fretting amplitude (Y_b) measured at a distance of 89 mm from the last point of contact (LPC) between the conductor and the suspension clamp, while 25% of the conductor Rated Tensile Strength (RTS) tension is maintained during the test.

The 3-D Drake conductor fretting fatigue assembly model shown in Figure 5 is built with high geometric precision using the Design Modeler of ANSYS Workbench 11.0 (2007). Due to the symmetry of the testing rig, only half of the assembly needs to be modeled with the suspension clamp center (SCC) taken as the origin. The model comprises 36 distinct solid bodies: 33 conductor helical wires, the suspension clamp body, one upper keeper and one U-bolt. The total length of the model is the half length of the suspension clamp up to the LPC, 95 mm, plus the reference test measurement distance at fretting amplitude, 89 mm, i.e. 184 mm.

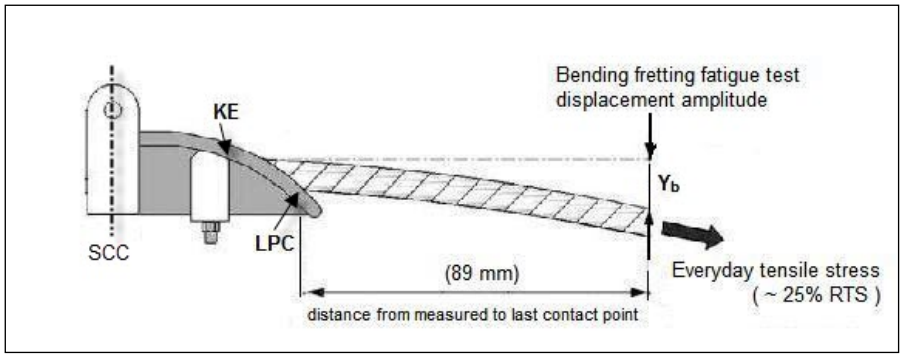

Figure 4: Schematic of conductor bending fretting fatigue testing rig

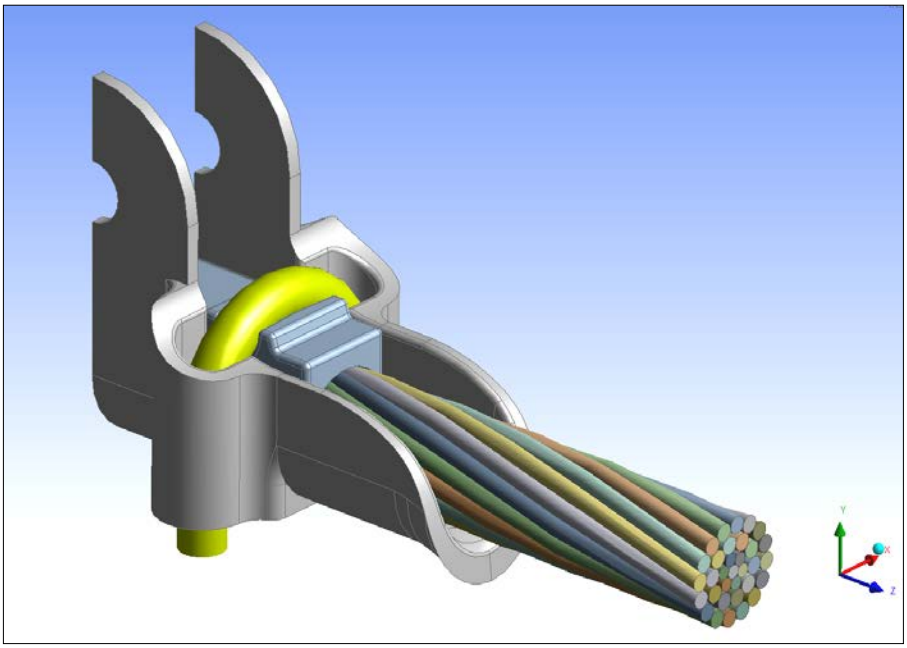

Figure 5: Drake conductor-clamp assembly solid model for fretting fatigue study

3. FINITE ELEMENT MODELING

Considering the particular features of the problem and the complex interfacial contact geometry among the conductor wires and the wires and clamp surface, the finite element method (FEM) is selected for detailed stress analysis. FEM has already gained widespread acceptability in industry during the last few decades. However, a number of modeling challenges are encountered in this application. This large nonlinear model exhibits very difficult convergence behaviour, which requires extensive numerical experiments as most program-supplied default parameters for numerical solution control and contact settings are inadequate. These issues have been resolved and are discussed in the paper.

3.1 Material Properties and Finite Element Selection

The material characteristics and element types used in the model are summarized in Table 1. Both types of conductor wires (aluminum alloy and aluminum–clad steel) are modelled with a nonlinear inelastic

constitutive law with large kinematics but small strains. The material non-linearities are defined using multi-linear fits of their experimental material curves obtained from a North American conductor manufacturer. As for the clamp components and U-bolt, they are assumed to be linear elastic. Although some experimental tests exposed that plastic deformations can occur on clamps, this study examines the inelastic response of the conductor wires only. For good solution accuracy with reduced computational cost, all components are discretized using solid elements with reduced-integration and hourglass control.

Table 1: Material characteristics and element types of the Drake fatigue model

Components	Material Characteristics		Element types
Outer & Inner wires	Aluminum Alloy	linear elastic to multi-linear plastic, large kinematics small strain	8-node 3-D hexahedral element
Core steel wires	Aluminum-clad Steel		8-node 3-D hexahedral element
Clamp body & Keeper	Aluminum	linear elastic, small kinematics small strain	4-node 3-D tetrahedral element
U-bolt	Galvanized Steel		8-node 3-D tetrahedral element

3.2 FE Meshing

Due to small anticipated fretting amplitudes of the order of 1.0 mm, a fine mesh is required to present the subtle stress variations inside the conductor strands and capture the stress gradients in the critical fretting contact regions. In addition, four layers of elements near the contact surfaces are necessary to obtain sufficient accuracy. However, the structural characteristics and the high nonlinearity of this problem (contact, friction and inelastic deformations) further complicate its mesh refinement. A very fine mesh in the regions of wire contact interfaces turns out to be problematic as the resulting deformed mesh under large kinematics becomes highly distorted (elements with singular Jacobian matrices) and hinder convergence. A number of numerical experiments were conducted and this trial-and-error process was very time-consuming since each trial had to perform a large-size nonlinear solution for the entire model. Finally, an optimal refined meshing scheme was achieved (see Table 2 and Figure 6) with sufficient solution accuracy while maintaining stable convergence provided that robust contact and solution control settings are carefully selected.

Table 2: An optimal meshing scheme for the Drake fatigue model

Meshing scheme	Mesh summary
Global element size = 0.5 mm	Total nodes = 323,731 Total solid elements = 309,805 Total contact elements = 274,478 Total elements = 585,147 * (* Include 864 spring elements to stabilize the nonlinear solution)
Outer & Inner wire face element size = 0.26 mm	
Outer & Inner wire edge divisions = 36 each edge	
Steel wire face element size = 0.45 mm	
Steel wire edge divisions = 20 each edge	
Element layers near wire contact surfaces = 4	
Longitudinal direction sweep division = 66 (Bias = 3)	

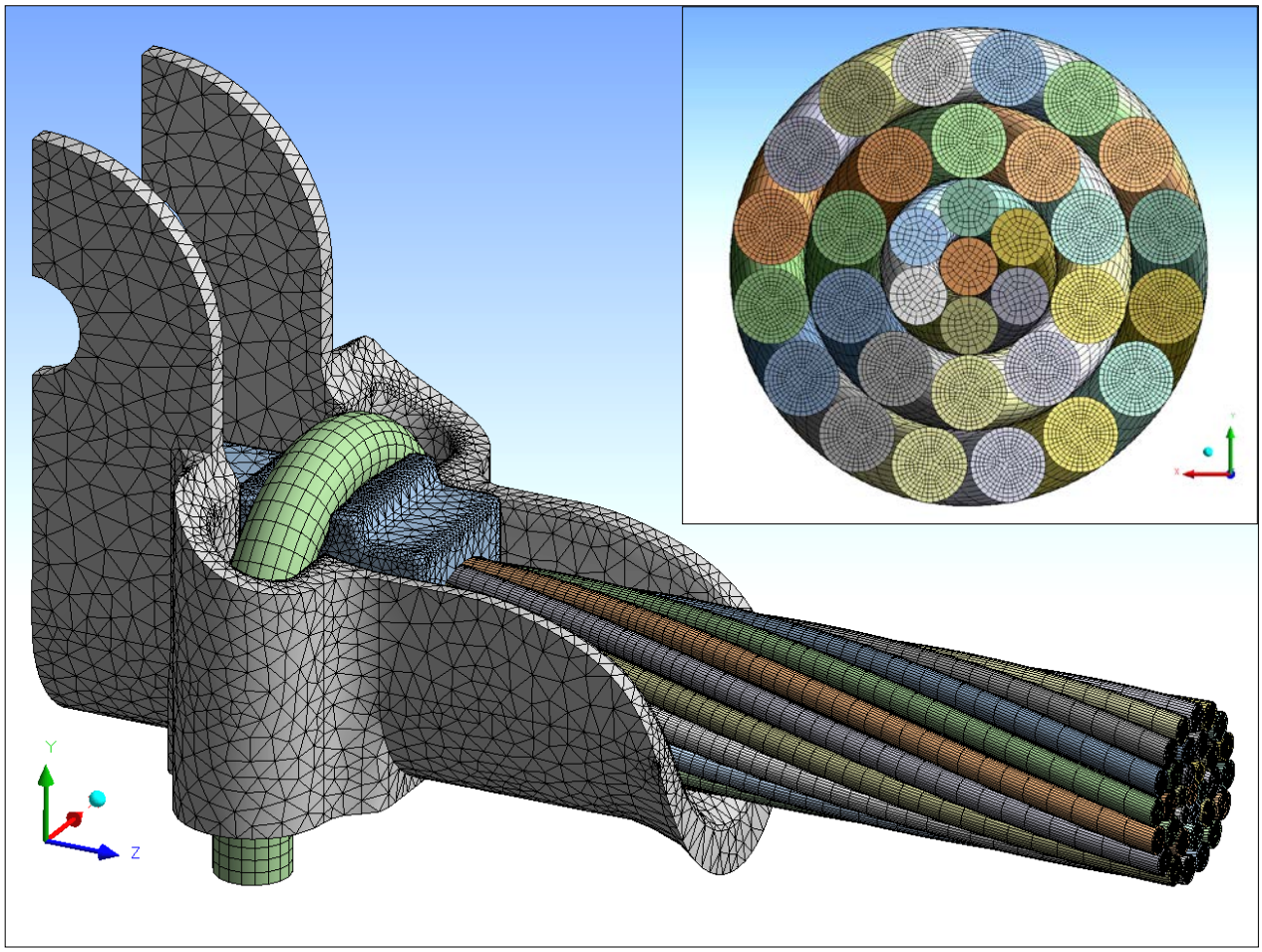

Figure 6: Finite element mesh of the Drake conductor-clamp assembly

3.3 Contact Condition Settings

The contact interactions amongst the different components of the entire assembly model are all defined as “flexible-to-flexible” deformable body contact, and “surface-to-surface frictional” contact types except between the Upper keeper and U-Bolt where “bonded contact” is defined to facilitate the computations. In total, 274,478 3-D 8-node surface-to-surface contact elements (CONTA174 in ANSYS) are employed. Coulomb friction law is used with different frictional coefficients assigned to all contact surfaces. After exploring all important contact properties, it was found that normal contact stiffness is the most critical parameter affecting both the convergence and accuracy of the calculated response. A large normal stiffness reduces contact penetrations and yields better accuracy but can cause ill-conditioning of the global stiffness matrix, leading to “oscillating” convergence and outright divergence. A small normal stiffness decreases solution accuracy and causes very slow convergence rate or even global divergence. Also, no uniform normal stiffness value can work for the whole model, and different values must be determined for each different contact regions to overcome the convergence difficulty. By trial-and-error, a set of optimal normal contact stiffness factors have been obtained for this particular problem, as shown in Table 3. Moreover, to achieve robust convergence, all normal and tangential contact stiffness terms are specified to be updated after each equilibrium iteration, based on the mean stress of the underlying elements, allowable penetrations, contact pressure, as well as slip. A parametric study was conducted on the ACSR Drake strength model where the coefficient of friction between the aluminum wires in all contact pairs was varied between 0.0 and 1.35. The results indicated that after the μ_s value increases above 0.57, the stress differences with different frictional coefficients are negligible. This conclusion

implies that the frictional coefficients will become insensitive to the stress status as long as the conductor aluminum wire surfaces are designed and kept in a dry and clean working condition.

Table 3: Contact settings used in the Drake fretting fatigue model

Contact region	Frictional coefficient (μ_s)	Normal contact stiffness factor	Resulting contact stiffness (N/mm^3)
Steel wires & Steel wires	0.60	0.15	2558
Inner wires & Inner wires	1.05	0.50	2861
Outer wires & Outer wires	1.05	0.50	2845
Steel wires 1-6 & Steel wire 0	0.60	0.20	3423
Steel wires 1-6 & Inner wires	0.45	0.40	2289
Inner wires & Outer wires	1.05	0.40	2288
Outer wires & Upper Keeper	1.05	0.25	1423
Outer wires & Clamp body	1.05	0.20	1138
Upper Keeper & U-Bolt	"Bonded"	0.042	11378

3.4 Multiple-step loading and boundary conditions

The applied loads comply with the bending fretting fatigue laboratory tests performed by Zhou et al. (1994, 1996), leading to a multiple load step analysis implemented sequentially to complete the entire load history for one bending fretting cycle. The complete load history consists of four load steps: (1) A clamping pressure from the U-bolt (47 N·m torque) is applied and held constant in the following steps, while symmetric displacement boundary conditions are applied on the clamp transverse symmetry plane (SCC) and fixed displacements are prescribed on the clamp fastener hole bottom plane to remove the rigid body movements of the system. (2) 25% RTS longitudinal conductor tension (34.65 KN) is defined and maintained constant afterwards. Using the "displacement-control" approach (Qi and McClure, 2010) that is based on the assumption of displacement compatibility for a short segment of a straight cable, an equivalent axial cable elongation of 0.2484 mm is applied as a prescribed axial displacement on the free-end surfaces of the conductor. Steps 1 and 2 constitute the pre-stressing stage of the fretting test. (3) A prescribed vertical displacement (Y_b) is gradually applied on the free-end surfaces of the conductor to simulate the imposed bending fretting amplitude induced by aeolian vibration. (4) The last step is to reduce the fretting amplitude to zero to complete the fretting cycle.

During the solution process, the time increment setting is a very sensitive control parameter to maintain a stable convergence process and also a significant driven factor to reduce the computational cost, which has to be adjusted to each different loading stages defined above. In effect, the time increments in this model must be set very small to avoid abrupt changes in the load increments; otherwise, either big oscillating normal contact forces or large contact penetrations could be induced that would jeopardize convergence. By trial and error, a set of optimal time step control settings are obtained (see Table 4).

Table 4: Time step settings in the Drake fretting fatigue model

Load Step	Initial time step	Min. time step	Max. time step
Step 1	0.010	0.001	0.020
Step 2	0.010	0.005	0.030
Step 3	0.010	0.010	0.050
Step 4	0.010	0.010	0.100

4. NUMERICAL SOLUTION TECHNIQUES

ANSYS Workbench 11.0 (64-bit) is used as the FE computing platform on a Dell Precision T5500 Workstation customized for this study. Solving this numerical model was difficult and very time-

consuming. Since there exists up to now no robust and efficient solver that can guarantee accuracy and convergence in all nonlinear solid mechanics problems (Wriggers, 2008), an optimal strategy may only be tailored to the physics and problem size of a specific application. Three-dimensional multi-body frictional contact exhibits a strong nonlinearity because both the normal and tangential contact stiffness change significantly with the changing contact status, and unpredictable sliding paths further complicate the analysis. After several numerical experiments, the Augmented Lagrangian contact algorithm was implemented within every load increment to enforce contact compatibility at the contact interfaces. It is a penalty-based method with penetration control using Lagrange multipliers and is reputed for its accuracy in frictional sliding contact analysis (Simo and Laursens, 1992).

As for the solution of the global nonlinear system equations, the full Newton-Raphson scheme is chosen for its robustness. For every load increment, a series of iterations for the system equilibrium need to be implemented by a linear equation solver, which plays a key role in the efficiency of the global solution process. Another consideration is that frictional contact generates an unsymmetric system stiffness matrix. Although a symmetrization algorithm is available in ANSYS to make use of the symmetric solvers, when frictional effects are substantial, the symmetric approximations cause a low rate of convergence. Based on the foregoing study, the Sparse Direct unsymmetric solver is selected. Finally, both force and displacement convergence criteria are used to ensure accuracy in the equilibrium iterations.

In addition, several convergence enhancement tools are activated within Newton-Raphson iterations, including automatic time stepping, time-step bisection and line search. Although very small load steps have been specified with minimum step size of 0.001 to ensure stability, “chattering” is still encountered during the computations, sudden spurious system stiffness changes leading to convergence difficulty. Therefore, to enhance numerical stability and prevent rigid-body motion, some weak spring elements are used with negligible stiffness to have no effect on the solution accuracy.

5. COMPUTATIONAL RESULTS

As stated earlier, this paper focuses on the numerical challenges for modeling a conductor-clamp system under fretting fatigue testing condition. Detailed discussions on the computational results, validations, as well as fatigue analysis are not be presented herein - see Qi (2013) for full details, while only some representative partial results under fretting amplitude of 1.3 mm are reported below.

5.1 Contact kinematics states

The computed contact kinematics states in the conductor fretting region show overall agreement with the experimental and field observations. “Partial slip contact” is clearly identified in the clamp mouth area on both the outer and inner layer wire contacting surfaces as some very small and local relative sliding occurs (Figures 7 and 8). Furthermore, the modeling results show that occurrences of partial slip contact may be accompanied by local plasticity on the fretting contact surfaces, as evidenced by the fretting marks in Figures 9 and 10. The “cross contact” between the inner and outer layers generates elliptical fretting marks due to the opposite lay angles of the contacting layers, which are much more critical than the very narrow band-shaped fretting marks from “parallel contact” among the wires of the same layers. These fretting mark distributions are also consistent with the ones in the “fretting chart” based on experimental observations (Zhou et al., 1994, 1996), and the marks reported in an ACSR field fatigue failure analysis by Azevedo, et al. (2009).

5.2 Von-Mises stresses at the Keeper Edge

The Von-Mises stress distribution in the conductor at the KE cross-section is shown in Figure 11. Due to the contact interactions, the stress field in the aluminum alloy wires exhibits a complex pattern, while the main load-carrying role of the steel wires is confirmed. The aluminum wires at KE have higher peak stresses than at LPC owing to the more severe multiaxial loading condition. In addition, mainly occurring in the “Upper Half-Section”, plasticity occurs on the contact surfaces of some wires on both the outer and inner layers, while the outer layer experiences higher peak stress and steeper stress gradient than the inner layer.

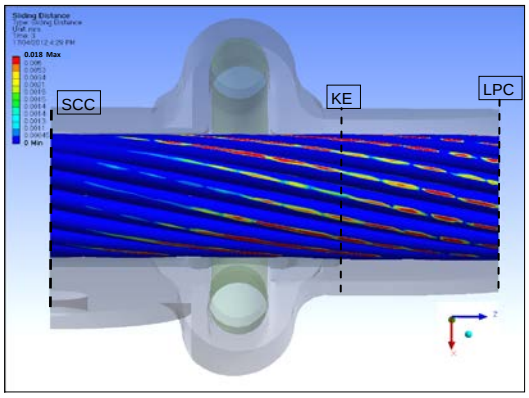

Figure 7: Partial slip contact state on outer layer

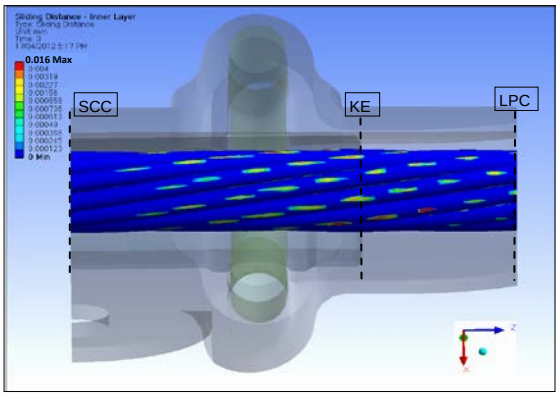

Figure 8: Partial slip contact state on inner layer

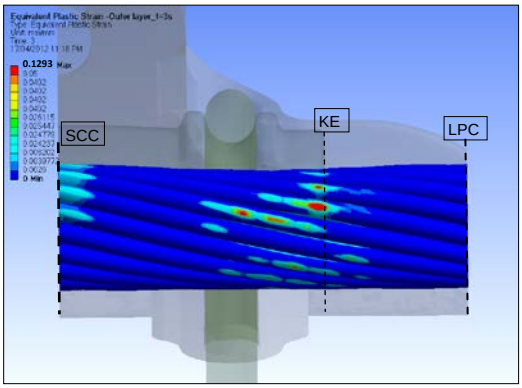

Figure 9: Fretting marks on outer layer

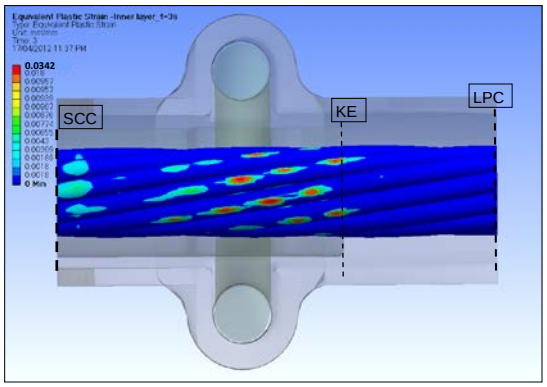

Figure 10: Fretting marks on inner layer

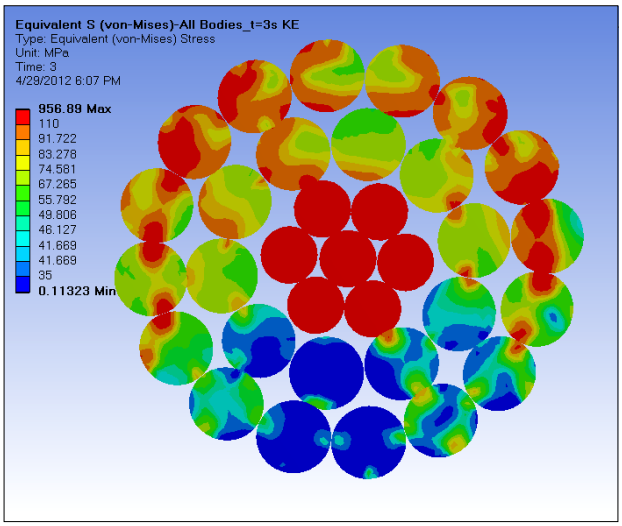

Figure 11: Drake conductor Von-Mises stress (S_{von}) at KE

5.3 Longitudinal stress

The conductor longitudinal stress (S_{zz}) is resulting from the combination effects of bending, longitudinal tension, friction, as well as the unbalanced internal torque. From Figure 12, it is clearly seen that the critical zone for conductor fretting fatigue is located in the suspension clamp mouth region between KE

and LPC. The fretting micro cracks mostly initiate at contacting surfaces under partial slip contact state, during which the longitudinal (axial) stress plays an essential role. Under the 25% RTS conductor tension, the nominal average axial stress of the aluminum wires is only about 59 MPa (Zhou et al., 1994, 1996), but with the occurrence of fretting, very high local stress concentrations are predicted.

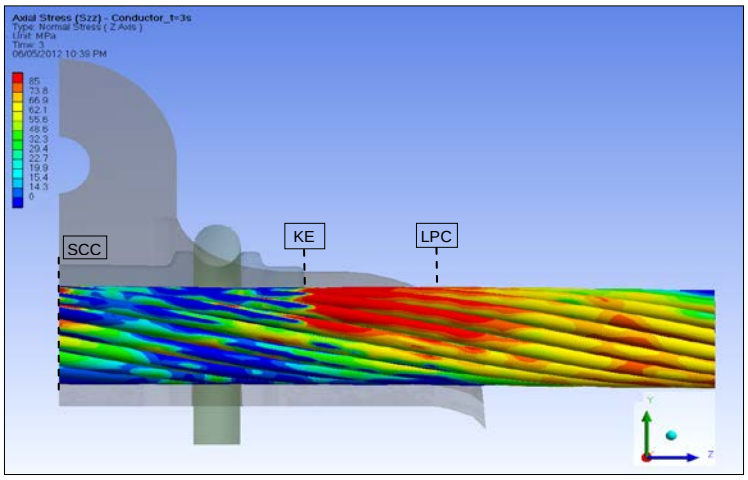

Figure 12: Longitudinal stress (S_{zz}) of Drake conductor

6. CONCLUSIONS

An accurate refined computational model for detailed stress analysis of an ACSR conductor under bending fretting fatigue has been constructed. The model incorporates the material nonlinearities of the aluminum components and the complex contact interactions of all the wires and the suspension clamp device. This model proved dependable for a better prediction of the complex conductor fretting fatigue behavior. Many numerical challenges have been overcome in the modeling process to obtain a robust convergence with sufficient solution accuracy.

7. REFERENCES

ANSYS Inc. 2007. *Theory Reference for ANSYS and ANSYS Workbench*. Canonsburg, PA, USA.

Azevedo, C.R.F., Henriques, A.M.D., Pulino Filho, A. R., Ferreira, J. L. A. and Araujo, J. A. 2009. Fretting fatigue in overhead conductors: Rig design and failure analysis of a Grosbeak aluminum cable steel reinforced conductor. *Engineering Failure Analysis*, 16: 136–151.

Qi, G. 2013. *Computational modeling for stress analysis of transmission line conductors under design and fretting fatigue conditions*. Dept. of Civil Eng. and Applied Mechanics, McGill University, Ph.D. Thesis.

Qi, G. and McClure, G. 2010. Computational Modeling for Stress Analysis of an Overhead Optical Ground Wire, *The CSCE 2nd International Structural Specialty Conference*, Winnipeg, Canada.

Simo, J.C. and Laursen, T. A. 1992. An Augmented Lagrangian Treatment of Contact Problems Involving Friction. *Computers and Structures,* 42 (1): 97-116.

Wriggers, P. 2008. *Nonlinear Finite Element Method*, Springer-Verlag, Berlin, Heidelberg, Germany.

Zhou, Z. R., Cardou, A., Goudreau, S., and Fiset, M. 1994. Fretting patterns in a conductor-clamp contact zone. *Fatigue and Fracture of Engineering Materials & Structures*, 17(6): 661–669.

Zhou, Z. R and Vincent, L. 1995. Mixed fretting regime. *Wear*, 181-183(2): 531-536.

Zhou, Z. R., Cardou, A., Goudreau, S., and Fiset, M. 1996. Fundamental investigations of electrical conductor fretting fatigue. *Tribology International*, 29(3): 221-232.